Supplementary Material

Pharmacokinetic Behaviors of Intravenously Administered siRNA in Glandular Tissues

Yuanyu Huang[a*], Qiang Cheng[a], Jia-Li Ji[b], Shuquan Zheng[a], Lili Du[a], Lingwei Meng[a], Yidi Wu[a], Deyao Zhao[a], Xiaoxia Wang[a], Li Lai[d], Huiqing Cao[a], Kai Xiao[d], Shan Gao[b], Zicai Liang[a,c*]

[a] Institute of Molecular Medicine, Peking University, Beijing 100871, China

[b] Suzhou Ribo Life Science Co. Ltd., Jiangsu 215300, China

[c] Collaborative Innovation Center of Chemical Science and Engineering (Tianjin), Tianjin 300072, China

[d] National Chengdu Center for Safety Evaluation of Drugs, State Key Laboratory of Biotherapy, Collaborative Innovation Center for Biotherapy, West China Hospital, Sichuan University, Chengdu 610041, China.

[*] Correspondence should be addressed to Y. Huang (yyhuang@pku.edu.cn, Tel: +86-10-62750683) or Z. Liang (liangz@pku.edu.cn, Tel./fax: +86-10-62769862)

Supplementary figure S1:

siRNA stability in mouse serum.

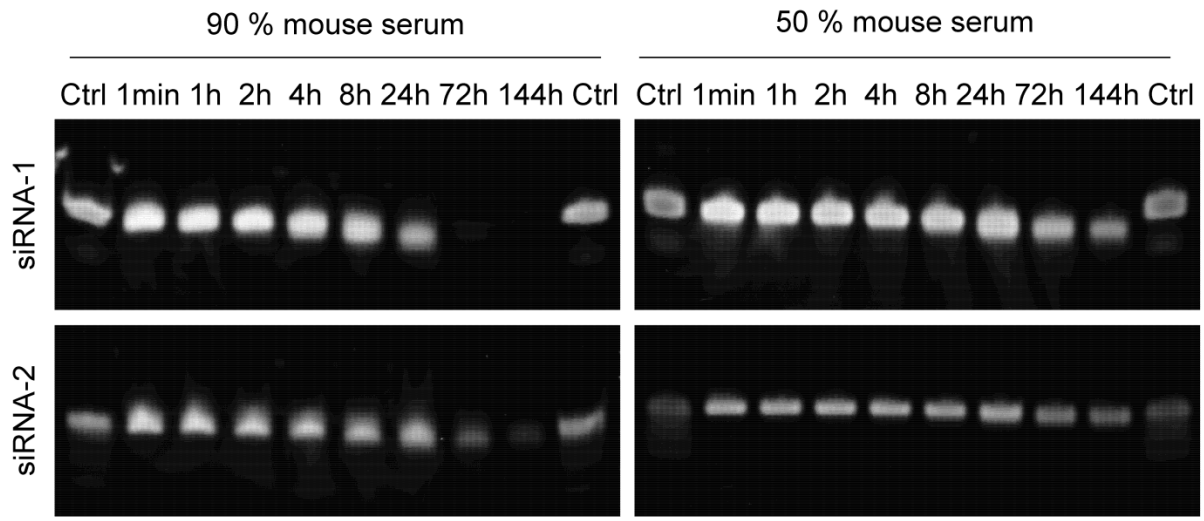

Figure S1. siRNA stability in mouse serum. siRNA-1 and siRNA-2 were incubated in mouse serum (90% and 50%, v/v) for desired time-frames, then separated in 12% native polyacrylamide gels to show the locations of siRNAs. It was demonstrated that both siRNA-1 and siRNA-2 were stable for more than 24 hours in mouse serum, and siRNA-2 remained in full length even has incubated for 144 hours (6 days). Ctrl, control siRNA without treatment.

Supplementary figure S2:

siRNA concentration-time curves for tissues without perfusion (6 time points)

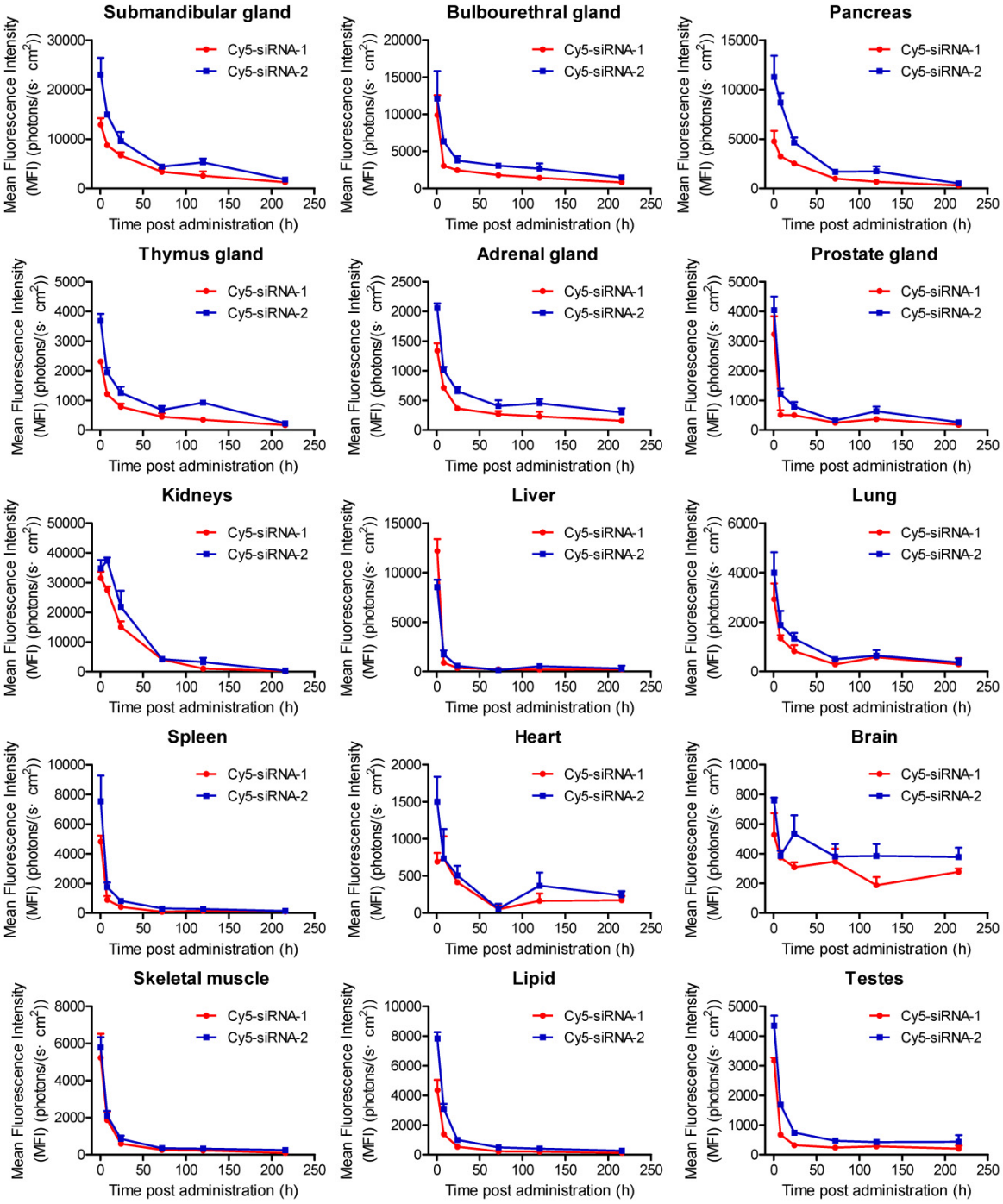

Figure S2. siRNA concentration-time curves for various tissues. Fluorescence signals of siRNAs (Cy5-labeled siRNA-1 and siRNA-2) were recorded at 0.5 h, 8 h, 24 h, 72 h, 120 h and 216 h post administration. The fluorescence images of whole bodies and isolated organs have been shown in figure 1a and figure 1b, respectively. Figure 1c represented the semi-quantitative analysis data of figure 1b, which displayed the MFIs of siRNAs in various tissues at certain time point. Based on the same original quantitative data, the dynamic attenuations of MFIs in certain tissue against the time changes were plotted and shown here.

Supplementary table S1:

AUCs of intravenously-administered naked siRNAs for tissues without perfusion (6 time points)

Tissues	Cy5-siRNA-1		Cy5-siRNA-2	
	AUC(0-t) {[photons/(s·cm^2)]·h}	AUC(0-∞) {[photons/(s·cm^2)]·h}	AUC(0-t) {[photons/(s·cm^2)]·h}	AUC(0-∞) {[photons/(s·cm^2)]·h}
Brain	62164.6	229364.0	88956.0	3628338.4
Submandibular gland	769295.4	877092.0	1236684.9	1470556.6
Pancreas	240778.2	258104.1	523580.9	584728.3
Bulbourethral gland	385705.1	531698.2	653551.6	994026.4
Prostate gland	81973.1	118952.7	128039.9	169188.5
Thymus gland	103578.4	123486.1	183938.6	227468.2
Adrenal gland	62576.5	104074.2	107671.4	179549.7
Heart	47435.2	57658.6	69630.5	133278.9
Lung	122856.4	165111.3	167600.8	207048.5
Liver	113067.3	149725.6	135909.8	179283.4
Spleen	60181.6	63525.5	118182.0	128538.3
Kidney	1239927.6	1263595.1	1768715.2	1797387.7
Lipid	84323.4	108203.7	169832.9	229416.1
Skeletal muscle	96856.2	108361.5	129773.4	192645.7
Testes	73541.1	111326.9	139246.1	208784.9

Table S1. AUCs of siRNA for tissues calculated with the data of figure S2 by DAS2.0 software. DAS2.0 is a professional pharmacokinetic analysis software. $AUC_{(0-t)}$, area under the siRNA concentration-time curves from time zero to the last quantifiable value; $AUC_{(0-\infty)}$: area under the siRNA concentration-time curves from time zero to infinity, which represents the total drug exposure over time.

Supplementary figure S3:

siRNA distribution in various tissues with perfusion before imaging

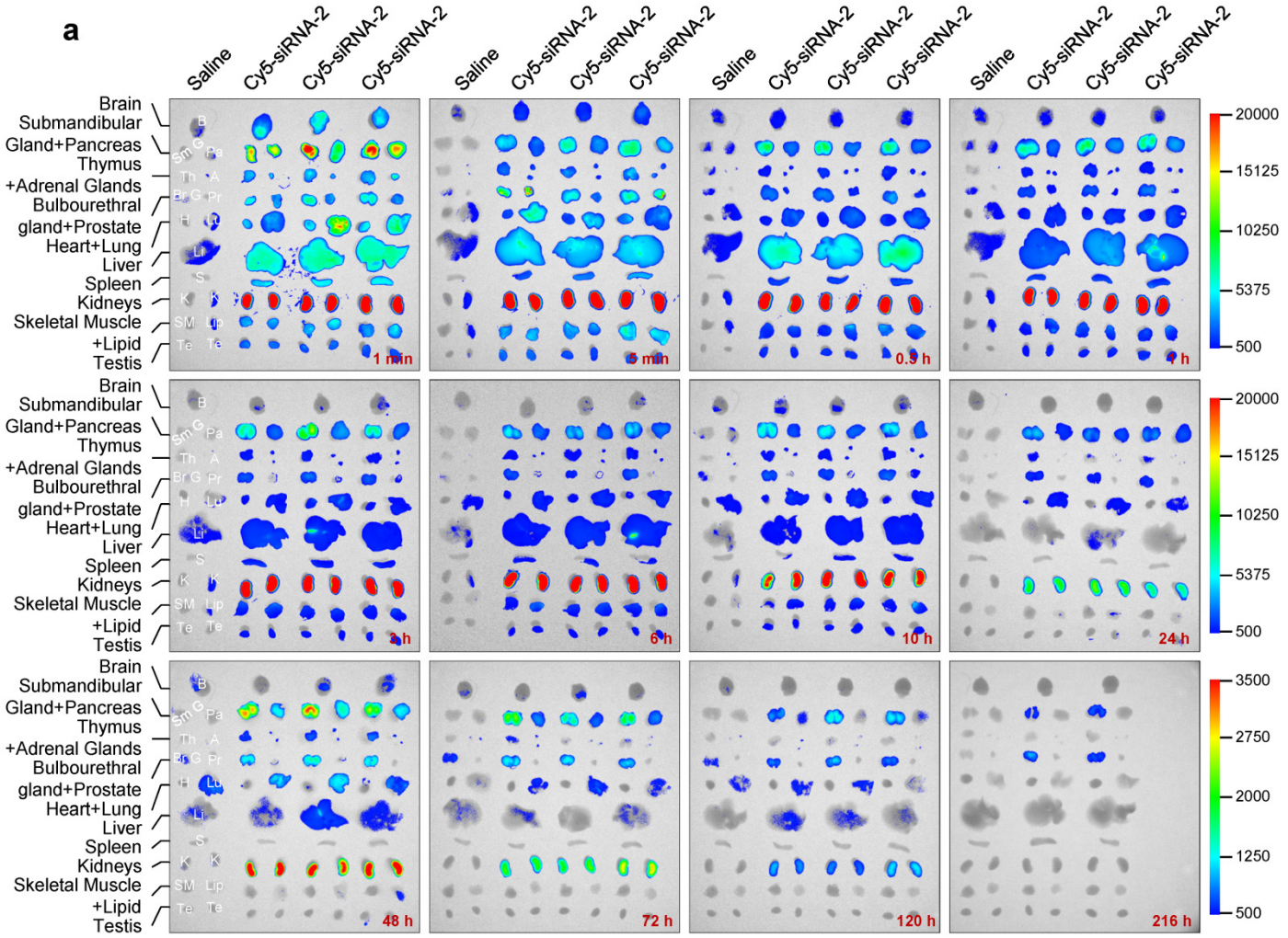

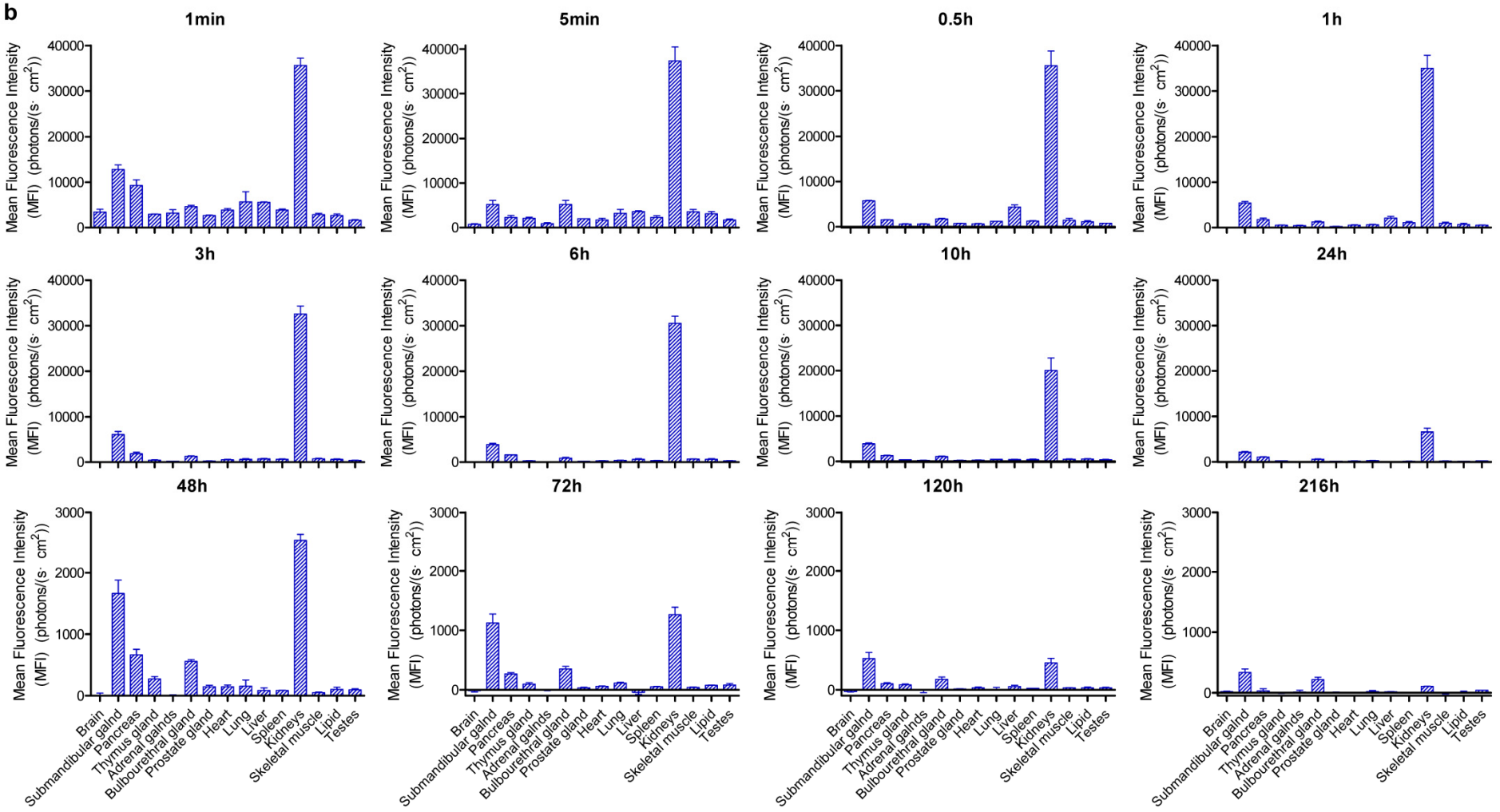

Figure S3. Fluorescence images of isolated tissues (a) and the corresponding semi-quantitative analysis data of these tissues (b) at indicated time points post administration. The blood was washed out of the body and perfused with 10 ml of saline before each time of fluorescence imaging. Data are mean ± SEM. N = 1 for saline-treated mice, and n = 3 for siRNA-treated mice at each time point, respectively.

Supplementary figure S4:

siRNA distribution in various tissues without perfusion before imaging

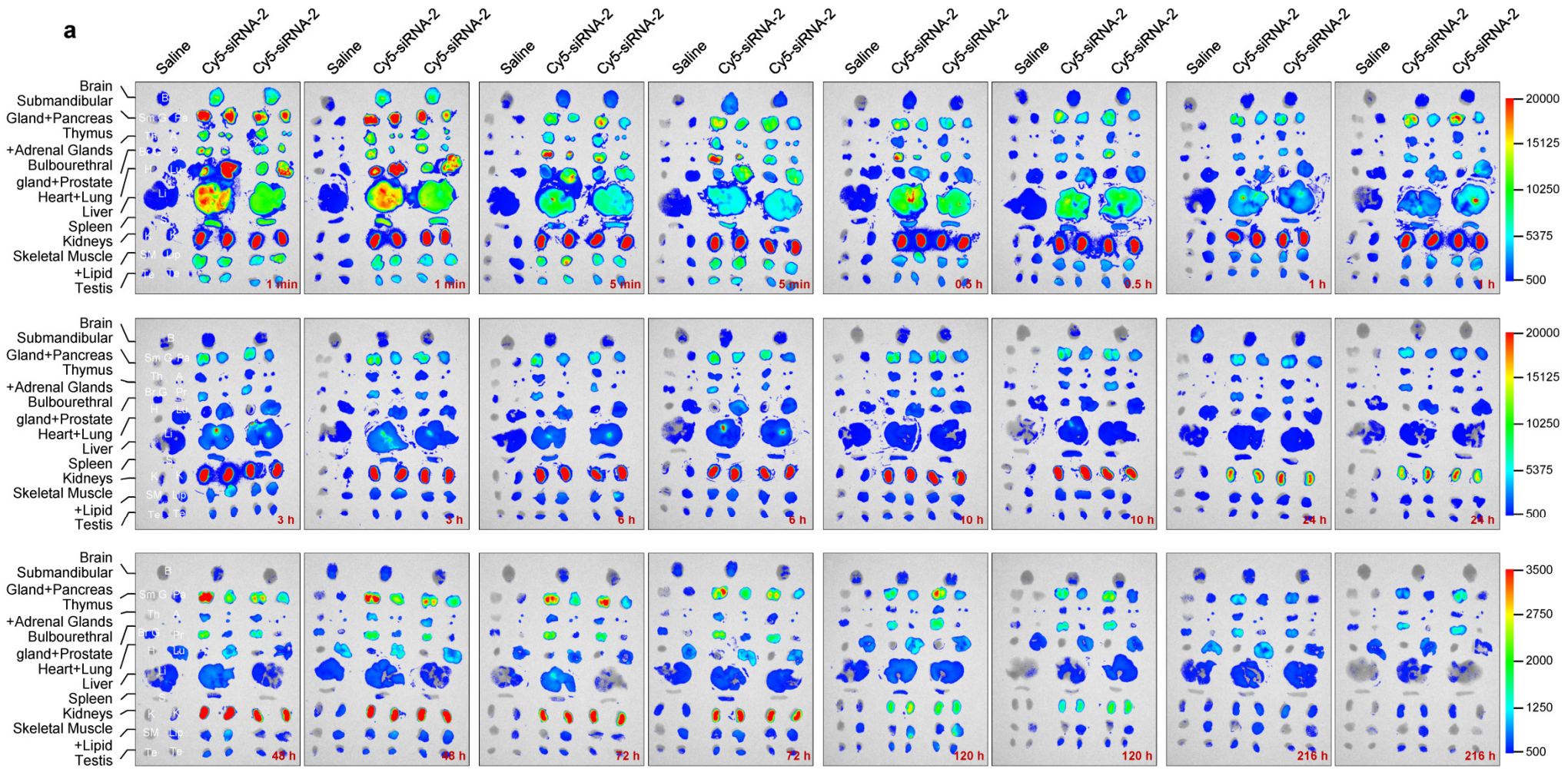

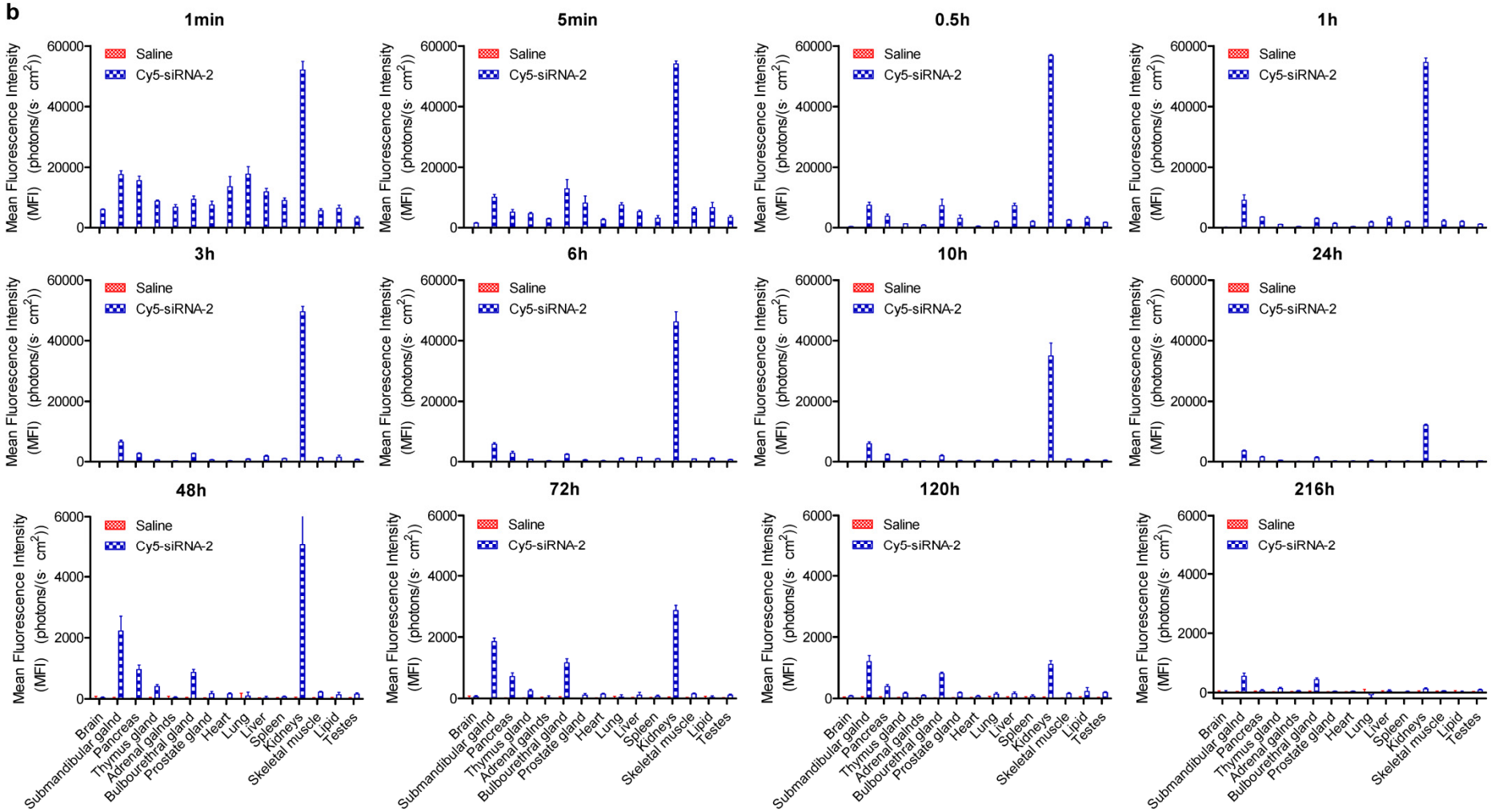

Figure S4. Fluorescence images of isolated tissues (a) and the corresponding semi-quantitative analysis data of these tissues (b) at indicated time points post administration. The blood was not perfused before imaging. Data are mean ± SEM. N = 2 for saline-treated mice, and n = 4 for siRNA-treated mice at each time point, respectively.

Supplementary figure S5:

siRNA concentration-time curves for tissues without perfusion (12 time points)

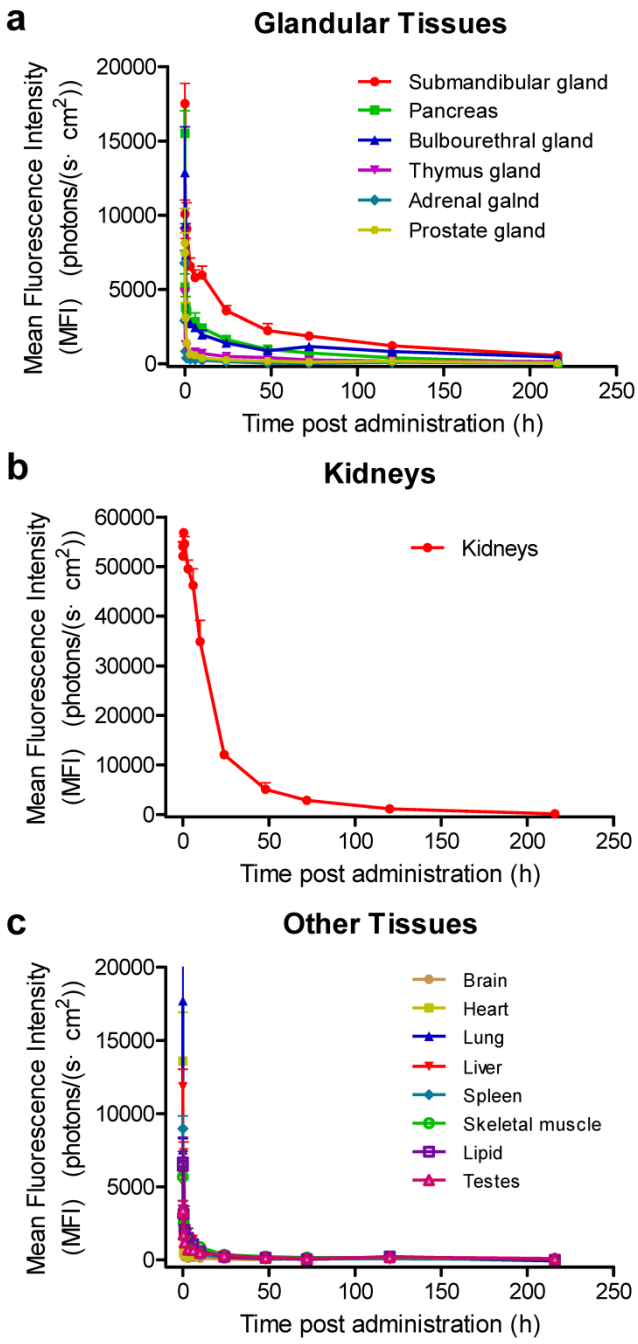

Figure S5. The dynamic changes of MFIs of Cy5-labeled siRNA-2 in various tissues. Based on the semi-quantitative data shown in figure S4b, siRNA concentration-time curves were plotted. The fluorescence intensities were recorded at 12 time points (1 min, 5 min, 0.5 h, 1 h, 3 h, 6 h, 10 h, 24 h, 48 h, 72 h, 120 h and 216 h) post administration. The blood of the mice was not washed out before imaging. Data are mean ± SEM (n = 4).

Supplementary table S2:

Half-lives and AUCs of intravenously-administered naked siRNAs for tissues without perfusion before imaging

Tissues	$t_{1/2\alpha}$ (h)	$t_{1/2\beta}$ (h)	$AUC_{(0-t)}$ {[photons/(s·cm^2)]·h}	$AUC_{(0-\infty)}$ {[photons/(s·cm^2)]·h}
Brain	0.030	5.258	3071.0	3154.0
Submandibular gland	0.033	27.111	315197.5	319176.9
Pancreas	0.024	25.273	131438.1	132385.5
Thymus gland	0.063	33.103	48454.2	50238.7
Adrenal glands	0.047	5.308	6284.6	6386.7
Bulbourethral gland	0.472	66.698	198693.1	233209.6
Prostate gland	0.333	36.956	32434.9	33489.5
Heart	0.026	43.109	25286.5	26537.9
Lung	0.045	5.906	19704.7	19973.7
Liver	0.004	2.075	20784.6	20952.2
Spleen	0.025	4.088	14768.6	14895.2
Kidney	13.700	13.701	1181605.9	1182524.5
Skeletal muscle	0.309	13.186	31871.2	31974.9
Lipid	0.290	7.580	23950.2	24062.5
Testes	0.379	23.232	27574.1	27810.3

Table S2. Pharmacokinetic parameters calculated with the data of figure S5 by DAS2.0 software. $t_{1/2\alpha}$, distribution half-life; $t_{1/2\beta}$, elimination half-life; $AUC_{(0-t)}$, area under the siRNA concentration-time curves from time zero to the last quantifiable value; $AUC_{(0-\infty)}$, area under the siRNA concentration-time curves from time zero to infinity, which represents the total drug exposure over time.

Supplementary figure S6:

***In vivo* distribution of lipofactamine 2000/siRNA complex.**

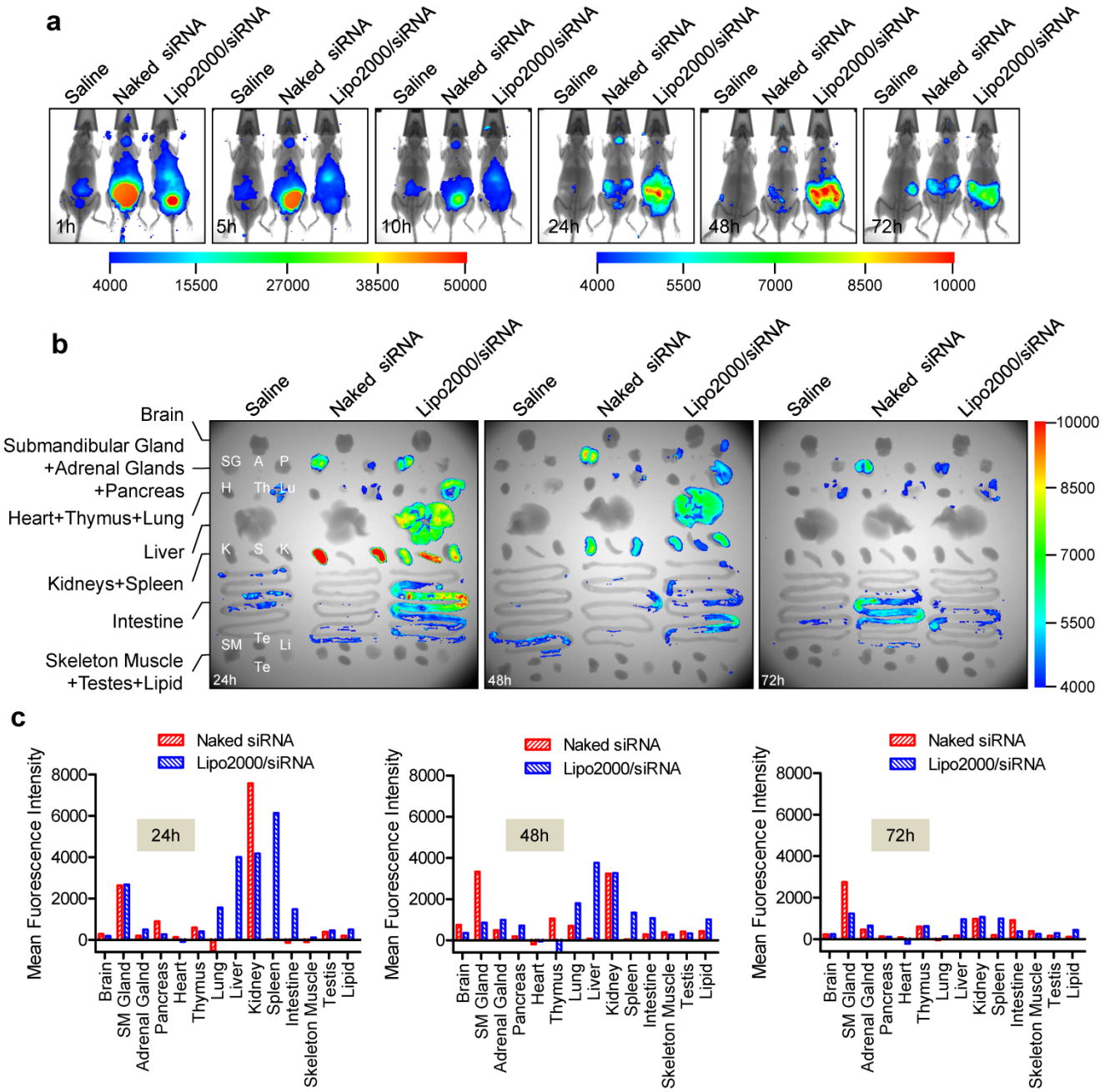

Figure S6. Biodistribution pattern of lipofectamine 2000/siRNA complex in C57BL/6 mice (1.0 mg/kg for siRNA). (a) Whole-body imaging at the indicated time points post intravenous administration. (b) Isolated organs examined by the imaging system at the end observation time points. (c) Quantitative analyses of (b) by using the included software of the imaging system. Data were normalized to corresponding tissues from saline-treated animals. Lipofectamine 2000/siRNA complex was prepared according to the manufacture's protocol. SG, submandibular gland; A, adrenal gland; P, pancreas; H, heart; Th, thymus gland; Lu, Lung; K, kidney; S, spleen; SM, skeleton muscle; Te, testes; Li, lipid.

Supplementary figure S7:

***In vivo* distribution of RGD10-10R/siRNA complex.**

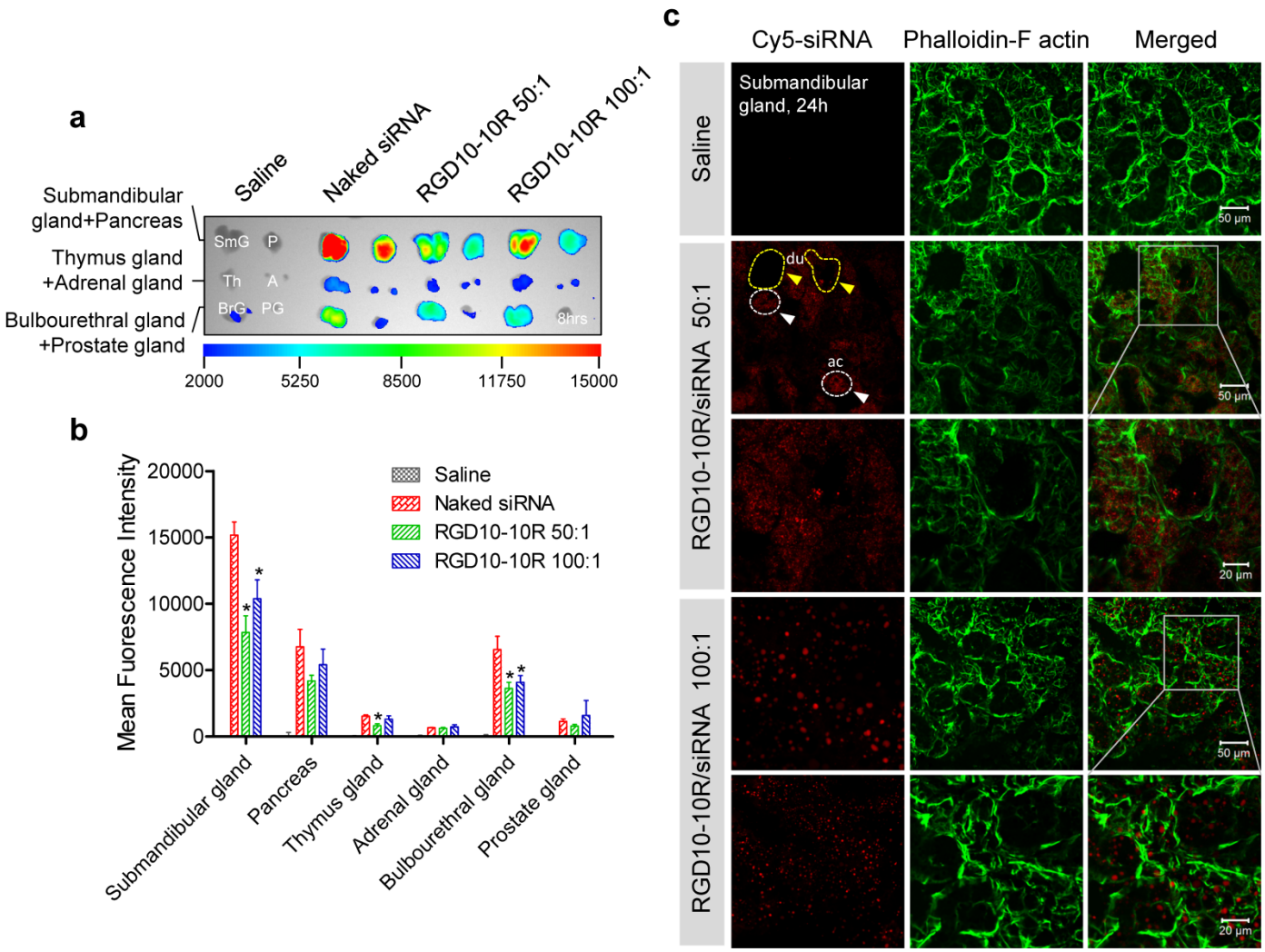

Figure S7. Biodistribution of RGD10-10R/siRNA complexes in C57BL/6 mice (2.5 mg/kg for siRNA) and their cellular localization in submandibular gland. RGD10-10R/siRNA complexes were prepared according to previous descriptions [1]. Briefly, RGD10-10R and siRNA powder were dissolved into 10-30 μg/μl and 1 μg/μl with DEPC (diethylpyrocarbonate)-treated water, respectively. Peptide and siRNA solutions were mixed directly according to different desired molar ratios (50:1 and 100:1). After electrostatic interaction for 15-20 min at room temperature, peptide/siRNA complexes were formed. Additional normal saline (NS) could be added to the complex solution to obtain the final formulations used for i.v. injection. *In vivo* imaging was performed at desired time points post administration. (a) Fluorescence imaging of isolated glands of the mice sacrificed at 8 hours post injection. (b) Mean fluorescence intensity of siRNA in the glands showed in (a). Data were normalized to corresponding tissues from saline-treated animals. Data were presented as mean ± SEM (n=3). *P < 0.05, vs. corresponding tissue from naked siRNA-treated mice. (c)

Confocal laser scanning microscopy (CLSM) images of the cryosections prepared with the submandibular glands collected at 24 hours post administration. Fluorescein isothiocyanate (FITC)-labeled phalloidin was used to stain F actin to show the rough cell outline. It was shown that RGD10-10R/Cy5-siRNA nanoparticles were detected in the acinar compartment (ac, white ellipses and arrowheads indicated), as well as in duct cells (du, as yellow irregularly circles and arrowheads pointed). For formulations of 'RGD10-10R/siRNA 50:1' and 'RGD10-10R/siRNA 100:1', magnified images (the lower panels) were acquired by zooming in the indicated areas of their parental images (the upper panels). The scale bars were shown in the lower right corners of the merged images. SmG, submandibular gland; P, pancreas; Th, thymus gland; A, adrenal gland; BrG, bulbourethral gland; PG, prostate gland.

Supplementary figure S8:

***In vivo* distribution of the siRNAs complexed with polymers of PEA and PEAG.**

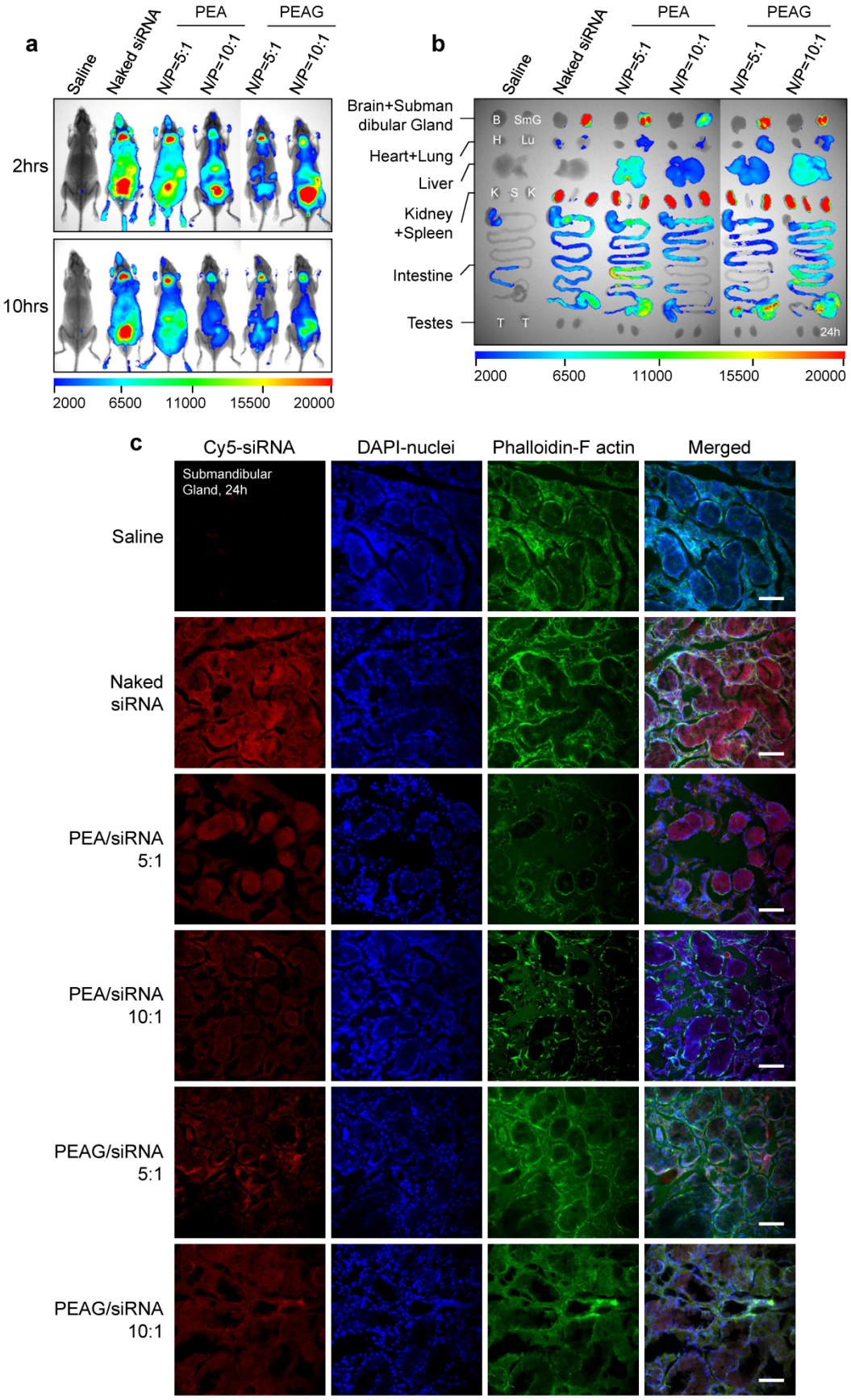

Figure S8. Biodistribution of PEA/siRNA and PEAG/siRNA complexes in C57BL/6 mice (2.5 mg/kg for siRNA) and their cellular localization in submandibular gland. According to the protocol

described previously [2], complexes of PEA/siRNA and PEAG/siRNA were developed by adding solution of PEGylated poly(2-aminoethyl methacrylate) (PEA) or guanidinylated PEGylated poly(2-aminoethyl methacrylate) (PEAG) into siRNA at different N/P ratios. The charge ratio (N/P) of polymers and siRNA was calculated as the molar ratio of the amino/guanidino groups (N) on polymer to the phosphate groups (P) on siRNA. Formulations were given into the mice by tail vein injection and *in vivo* imaging was performed at indicated time points (a). Mice were sacrificed at 24 hours post injection and isolated organs were checked again by fluorescence imaging (b), followed by cryosection preparation and confocal observation (c). DAPI and FITC-labeled phalloidin were used to stain nuclei and F actin (to show the rough cell outline), respectively. It seems that PEA/siRNA and PEAG/siRNA nanoparticles primarily localized in the acinar compartment. Scale bar: 50 μm. B, brain; SmG, submandibular gland; H, heart; Lu, lung; K, kidney; S, spleen; T, testes.

Supplementary figure S9:

***In vivo* distribution of PDMAEMA/siRNA complexes.**

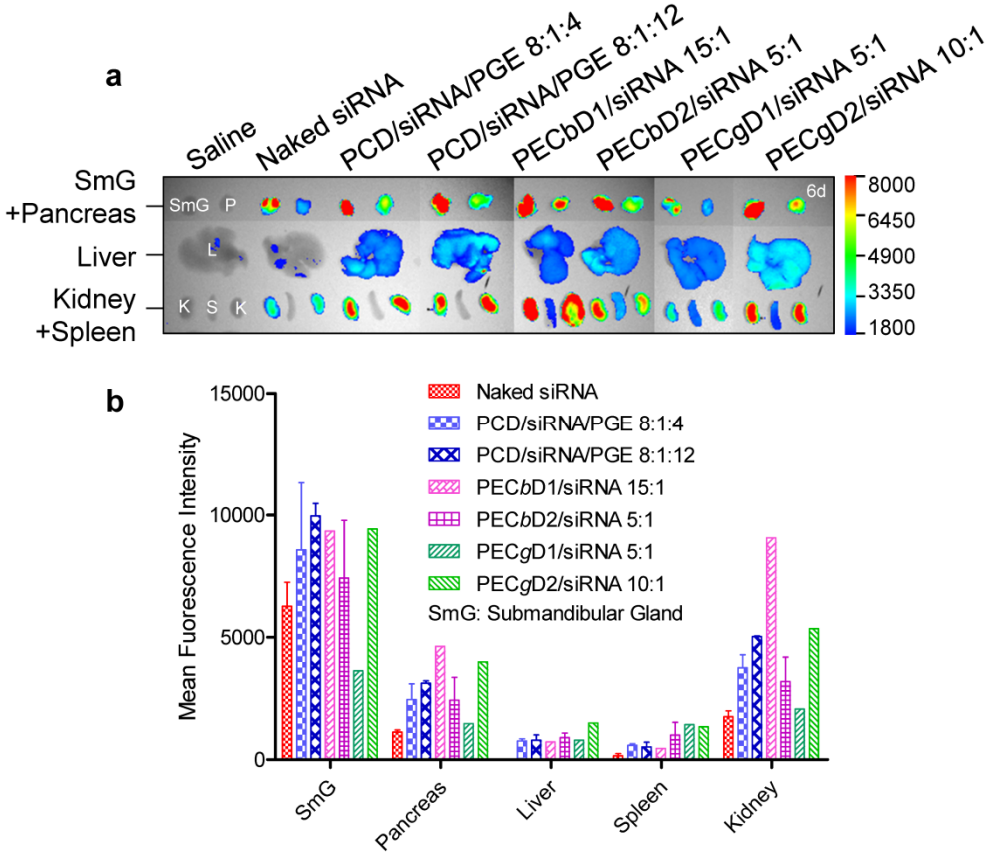

Figure S9. Biodistribution of siRNAs complexed with various PDMAEMA-derived materials in C57BL/6 mice (2.5 mg/kg for siRNA). Several PDMAEMA (poly(N, N-dimethylaminoethyl methacrylate))-based siRNA complexes were prepared as described previously [3, 4]. Briefly, We first developed binary complexes (PCD/siRNA) with polycaprolactone-graft-poly(N, N-dimethylaminoethyl methacrylate) (PCL-*g*-PDMAEMA, PCD) nanoparticles (NPs) and siRNA; and then made ternary complexes (PCD/siRNA/PGE) by coating polyglutamic acid-graft-poly(ethylene glycol) (PGA-*g*-mPEG, PGE) onto the binary complexes. The ratios following the complexes represented the charge ratio (N/P/C) of polymers and siRNA, which was calculated as the molar ratio of the amino groups (N) on PCD to the phosphate groups (P) on siRNA and the carboxyl groups (C) on PGE. Similarly, complexes of siRNA and PEC*b*D1, PEC*b*D2, PEC*g*D1 or PEC*g*D2 were prepared at various N/P ratios. Here, the N/P ratios represented the molar ratios of the amino groups (N) on PEC*b*D1, PEC*b*D2, PEC*g*D1 or PEC*g*D2 to the phosphate groups (P) on siRNA. Formulations were given into the mice by tail vein injection. (a) Fluorescence imaging of several organs isolated at 144 hours (6 days) post administration. (b) Quantitative analyses of (a) were performed with a included molecular imaging software package. SmG, submandibular gland; P, pancreas; L, liver; K, kidney; S, spleen.

Supplementary figure S10:

Pancreas cryosections of PDMAEMA/siRNA complexes-treated mice

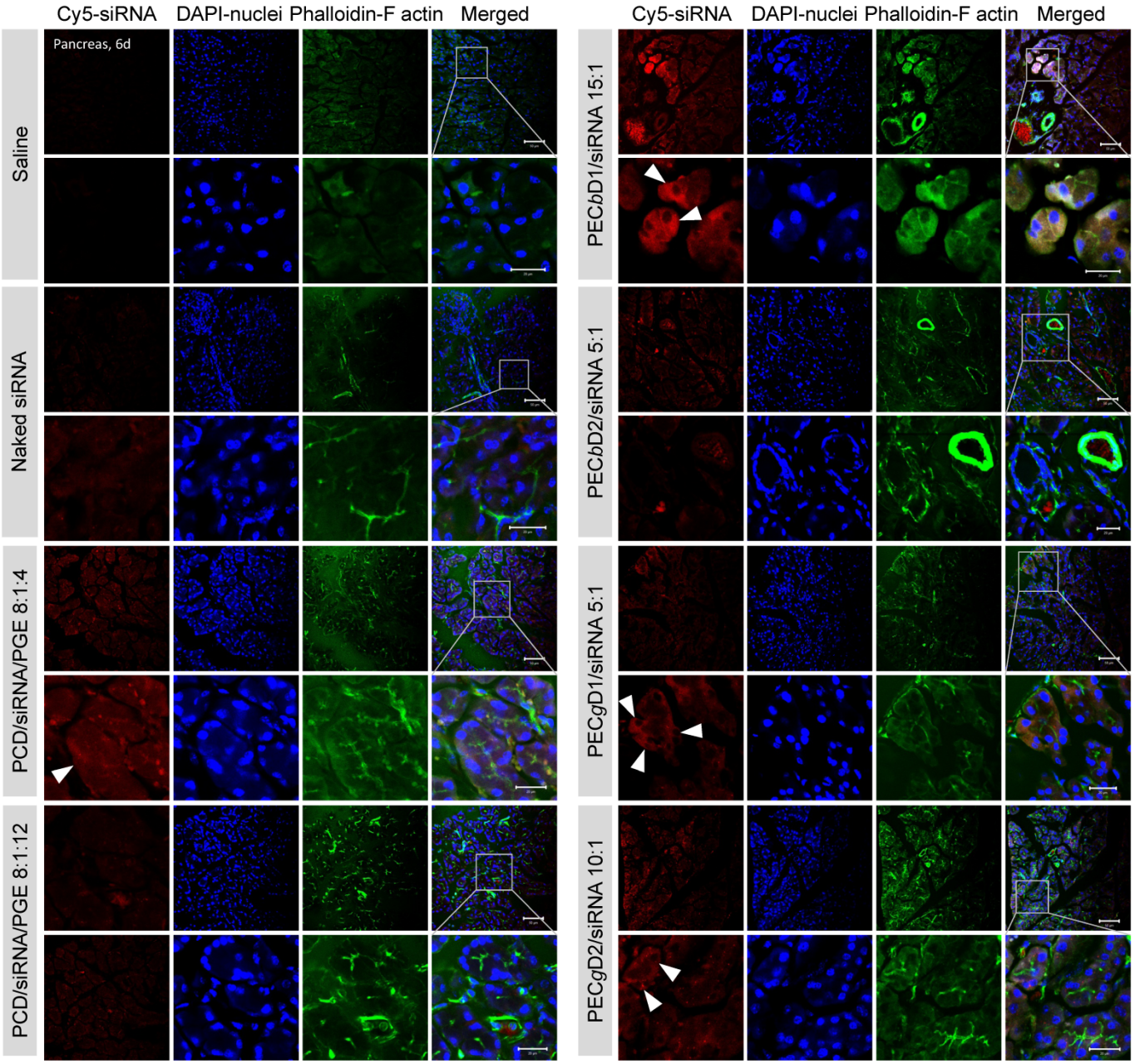

Figure S10. Confocal laser scanning microscopy (CLSM) images of the cryosections prepared with the pancreases of PDMAEMA/siRNA complexes-treated mice. DAPI and FITC-labeled phalloidin were also used to stain nuclei and F actin (to show the rough cell outline), respectively. For each field of each formulation, magnified images (the lower panels) were acquired by zooming in the indicated areas of their parental images (the upper panels). The scale bars of the parental images and magnified images were 50 μm and 20 μm, which were shown in the lower right corners of the merged images, respectively. It was shown that, siRNAs have been delivered into the cytoplasm of pancreas for sevral complexes, such as 'PCD/siRNA/PGE 8:1:4', 'PEC*b*D1/siRNA 15:1', 'PEC*g*D1/siRNA 5:1' and 'PEC*g*D2/siRNA 10:1', as the arrowheads indicated.

Supplementary figure S11:

***In vivo* distribution of dendrimer G5/siRNA complex.**

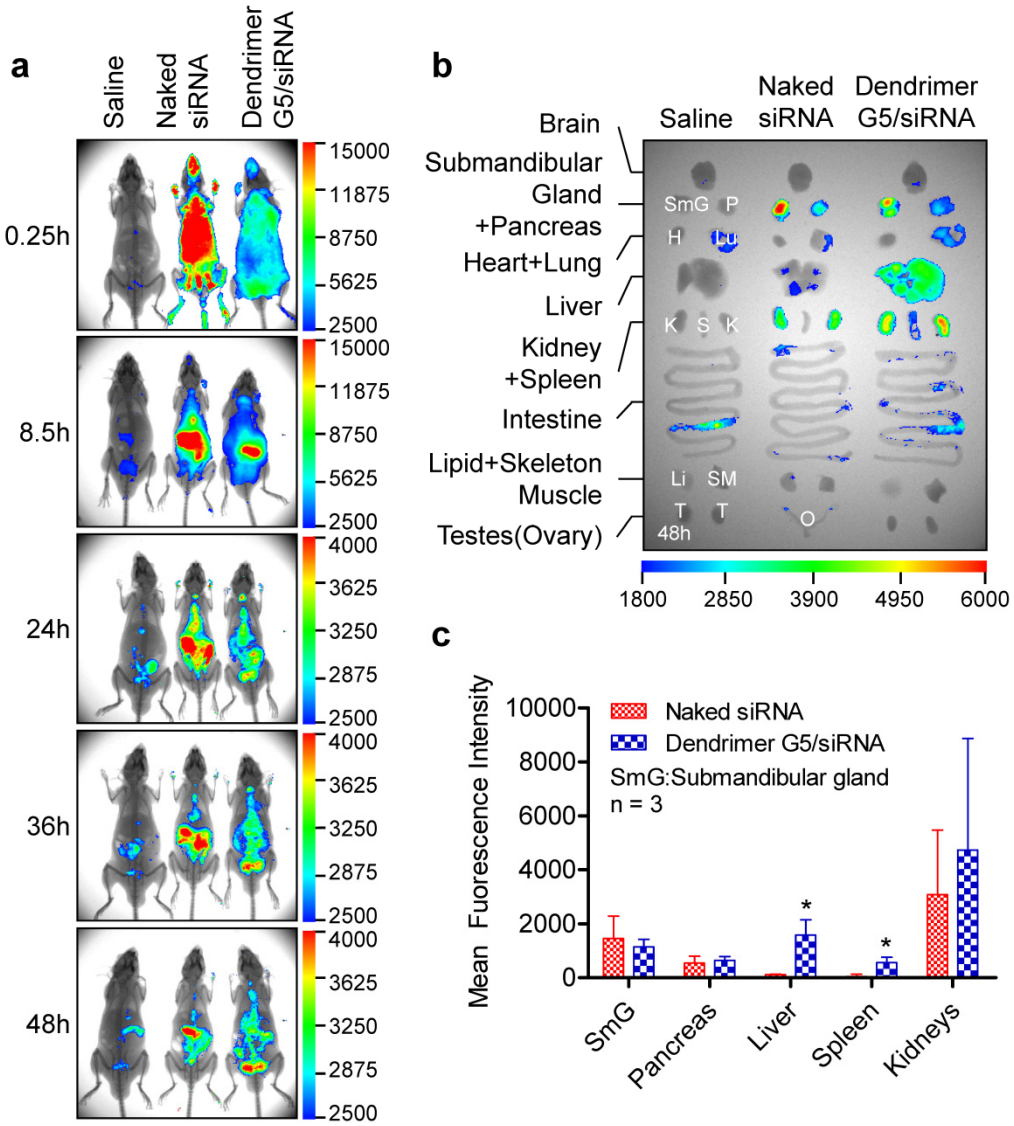

Figure S11. *In vivo* distribution of dendriemr G5/siRNA complexes in C57BL/6 mice (0.3 mg/kg for siRNA). Dendriemr G5/siRNA complex was prepared according to the protocol described previously [5] with minor modification. Dendrimers G5 were diluted to an appropriate concentration in phosphate-buffered saline buffer (pH 7.4) and the experimental siRNAs were diluted with H_2O. Both solutions were mixed at N/P (=[total end amines in cationic dendrimer]/[phosphates in siRNA]) ratio 10:1 and incubated at 37 °C for 30 minutes in phosphate-buffered saline buffer. Then formulations (saline, naked siRNA and G5/siRNA complex) were intravenously injected into the mice, followed by fluorescence recording with *in vivo* imaging system. (a) Whole body imaging at given time points. (b) Fluorescence detection of isolated main organs of mice at the final observation time point. (c) Quantitative analyses of (b). The data were normalized to corresponding tissues from saline-treated animals. Each bar represents the mean ± SEM of three independent

experiments. *P < 0.05, vs. corresponding tissue from naked siRNA-treated mice. SmG, submandibular gland; P, pancreas; H, heart; Lu, lung; K, kidney; S, spleen; Li, lipid; SM, skeleton muscle; T, testes; O, ovary.

Supplementary figure S12:

Cryosections of submandibular gland and pancreas of dendrimer G5/siRNA-treated mice.

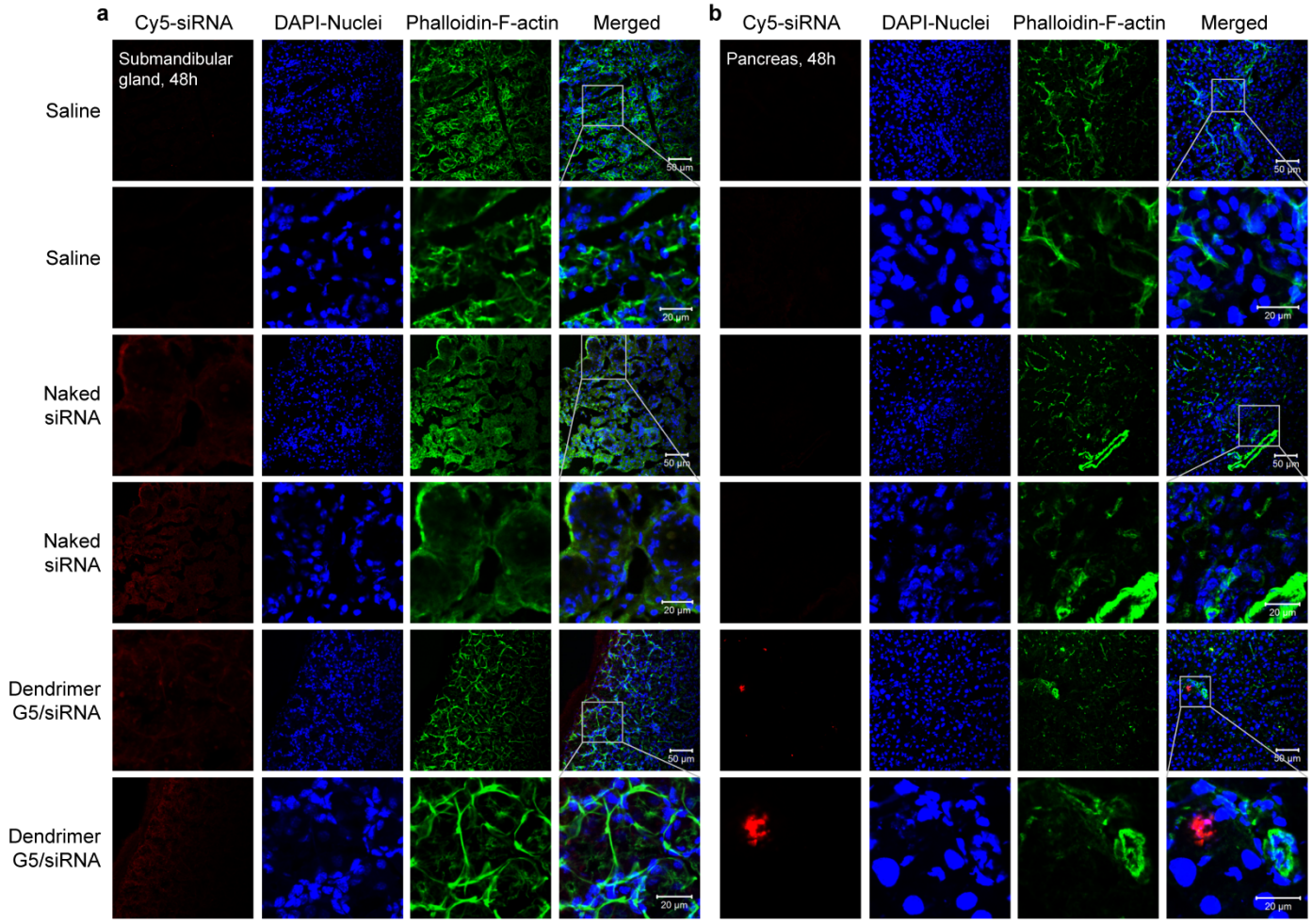

Figure S12. Confocal laser scanning microscopy (CLSM) images of the cryosections prepared with the submandibular gland (a) and pancreas (b) of dendrimer G5/siRNA complex-treated mice. DAPI and FITC-labeled phalloidin were also used to facilitate the observation. Enlarged images (the lower panels) were showed below the corresponding parental images (the upper panels) for each treatment. The scale bars of the parental images and magnified images were 50 µm and 20 µm, which were shown in the lower right corners of the merged images, respectively. It was observed that the fluorescence signals from the submandibular gland of the mice treated with naked and formulated siRNA were stronger than that from the pancreas of the same animal, which was in line with the MFI data of isolated organs (figure S12b-c).

Supplementary table S3

Physicochemical properties of carrier-encapsulated siRNA formulations

Formulation	Ratio type	Size (d, nm)	Zeta potential (mV)
AD/siRNA 5:1	N/P	376.00 ± 14.57	19.27 ± 0.32
AD/siRNA 10:1	N/P	185.00 ± 13.86	24.17 ± 0.21
Lipofectamine 2000/siRNA	N.A.	140.5 ± 15.27	24.40 ± 7.01
RGD10-10R/siRNA 50:1	Molar ratio	116.86 ± 61.90	21.40 ± 7.92
RGD10-10R/siRNA 100:1	Molar ratio	144.51 ± 39.82	20.08 ± 2.69
PEA/siRNA 10:1	N/P	258.30 ± 3.82	3.39 ± 0.23
PEAG/siRNA 10:1	N/P	207.80 ± 64.71	3.68 ± 3.30
PCD/siRNA/PGE 8:1:4	N/P/C	185.50 ± 7.35	18.40 ± 0.42
PCD/siRNA/PGE 8:1:12	N/P/C	182.00 ± 0.71	1.49 ± 0.91
PEC*b*D1/siRNA 15:1	N/P	119.80 ± 6.93	6.31 ± 0.43
PEC*b*D2/siRNA 5:1	N/P	84.70 ± 9.83	3.67 ± 0.55
PEC*g*D1/siRNA 5:1	N/P	131.80 ± 16.83	5.48 ± 0.45
PEC*g*D2/siRNA 10:1	N/P	132.75 ± 1.91	12.63 ± 0.76
Dendrimer G5/siRNA 10:1	N/P	107.96 ± 2.24	18.15 ± 0.92

Table S3. Physicochemical properties of carrier-encapsulated siRNA formulations. N/P, the molar ratios of the amino groups (N) on carrier to the phosphate groups (P) on siRNA; N/P/C, the molar ratio of the amino groups (N) on PCD to the phosphate groups (P) on siRNA and the carboxyl groups (C) on PGE; molar ratio, the molar ratio of peptide to siRNA; N.A., not available. N = 2-5.

References:

1. Huang Y, Wang X, Huang W, Cheng Q, Zheng S, Guo S, et al. Systemic Administration of siRNA via cRGD-containing Peptide. Sci Rep. 2015; 5: 12458.

2. Cheng Q, Huang Y, Zheng H, Wei T, Zheng S, Huo S, et al. The effect of guanidinylation of PEGylated poly(2-aminoethyl methacrylate) on the systemic delivery of siRNA. Biomaterials. 2013; 34: 3120-31.

3. Huang Y, Lin D, Jiang Q, Zhang W, Guo S, Xiao P, et al. Binary and ternary complexes based on polycaprolactone-graft-poly (N, N-dimethylaminoethyl methacrylate) for targeted siRNA delivery. Biomaterials. 2012; 33: 4653-64.

4. Lin D, Huang Y, Jiang Q, Zhang W, Yue X, Guo S, et al. Structural contributions of blocked or grafted poly(2-dimethylaminoethyl methacrylate) on PEGylated polycaprolactone nanoparticles in siRNA delivery. Biomaterials. 2011; 32: 8730-42.

5. Zhou J, Neff CP, Liu X, Zhang J, Li H, Smith DD, et al. Systemic administration of combinatorial dsiRNAs via nanoparticles efficiently suppresses HIV-1 infection in humanized mice. Mol Ther. 2011; 19: 2228-38.